J. Fluid Mech. (1981), *vol.* 107, *pp.* 201–220
Printed in Great Britain

On the mixing of a rectangular jet

By A. KROTHAPALLI, D. BAGANOFF AND K. KARAMCHETI

Joint Institute for Aeronautics and Acoustics,
Stanford University, Stanford, California 94305

(Received 6 November 1979 and in revised form 28 July 1980)

Results of hot-wire measurements in an incompressible rectangular jet issuing into a quiet surrounding at ambient conditions are presented. The quantities measured include distributions of mean velocity and the turbulence shear stresses in the two central planes of the jet at stations up to 115 widths (small dimension of the nozzle) downstream of the nozzle exit. The flow field of the jet was found to be characterized by the presence of three distinct regions, defined by the axial mean velocity decay, which are referred to as: a potential core region, a two-dimensional-type region, and an axisymmetric-type region. The onset of the axisymmetric region occurs at a downstream location where the two shear layers from the short edges of the nozzle meet. In the central plane which contains the small dimension of the nozzle, similarity was found both in the mean velocity and shear stress profiles beyond 30 widths downstream of the nozzle exit; however, profiles of r.m.s. velocity show similarity in the second but not the third region. The mean velocity, shear stress and r.m.s. velocity profiles in the central plane containing the long dimension of the nozzle do not show geometrical similarity.

1. Introduction

Most previous investigations in turbulent jets were carried out on two-dimensional or axisymmetric jets. A considerable amount of experimental data is available in the literature to define the structure and development of the flow fields of these jets (Everett & Robins 1978; Gutmark & Wygnanski 1976; Hinze 1976; Rajaratnam 1976; Schlichting 1968; Townsend 1976; Wygnanski & Fiedler 1969; and others). However, few experiments have been carried out on a rectangular jet of moderate aspect ratio with the degree of thoroughness found in either of the above two classes of jets. Early work on such jets was done at the Polytechnic Institute of Brooklyn by Sforza and his co-workers (Sforza, Steiger & Trentacoste 1966; Trentacoste & Sforza 1967). Their experimental study was limited to the measurement of gross properties of the jet because of their use of the Pitot tube. Their experiments revealed that the flow field of a rectangular jet was characterized by the presence of three distinct regions as defined by the decay of the square of the mean axial velocity along the axis of the jet. Discussion of these regions is deferred to § 3 of this paper. The mean velocity and temperature profiles of rectangular jets having different aspect ratios and nozzle geometries were measured by Sfeir (1976) using hot-wire anemometry. He drew attention to the effect of nozzle inlet geometry on the development of a jet. Some measurements of heated rectangular jets were reported by Sforza & Stasi (1977), and

these indicated that the conditions of the nozzle exit flow play a large role in the initial development of the jet. Recently Sfeir (1978) reported measurements of some turbulence quantities, using hot-wire anemometry, for nozzles of three different aspect ratios (10, 20, 30), each having two different inlet geometries, namely an orifice plate in one case and a long channel in the second. In the plane containing the long dimension of the nozzle, only profiles of mean and r.m.s. intensity of the axial component of velocity were obtained. Except for the description of the nozzle exit shapes, no further information was given of the flow nature, such as the boundary layer and the mean velocity profile, at the exit.

McGuirk & Rodi (1977) and Bobba & Ghia (1979) attempted to calculate the flow field for a rectangular jet using the two-equation turbulence model consisting of those for the turbulent kinetic energy and its rate of dissipation. They were able to calculate some of the observed features but noted that the conditions at the nozzle exit play a dominant role in the development of the flow and that these conditions must be clearly specified in experiments for comparison with calculations to be meaningful.

For purposes of comparison with prediction of numerical calculations, the desired conditions at the exit of a rectangular nozzle are a top-hat mean velocity profile with a known turbulence level and of boundary-layer type. A jet issuing from a sharp-edged orifice (Sforza *et al.* 1966; Sfeir 1976) exhibits a vena-contracta effect which unduly complicates the initial conditions for numerical modelling. Likewise, the mean velocity profile produced by a long channel (Sfeir) differs considerably from the profile found in practical applications such as thrust augmenting ejectors for short take-off and landing aircraft and certain jet engines where information on rectangular jets is needed. The nozzle employed in the present investigation was designed to produce a top-hat mean velocity profile with laminar boundary layer. In light of the above considerations, further systematic investigations on structure of rectangular jets of moderate aspect ratios with well-defined initial conditions are undertaken.

The characteristics of the flow field depend upon the aspect ratio (AR) of the nozzle, inlet geometry of the nozzle, the type of exit velocity profile, the magnitude of the turbulence intensity at the exit plane of the nozzle, the Reynolds number at the nozzle exit, and condition of the ambient medium into which the jet is issuing. In the present investigation, a nozzle of aspect ratio 16·7 was chosen. The inlet geometry of the nozzle was designed specifically to obtain a low turbulence level at the exit plane. The velocity profile at the exit plane of the nozzle was flat with a laminar boundary layer at the walls. A mean velocity of 60 m s^{-1} was maintained at the exit plane of the nozzle. This resulted in a Reynolds number of $1{\cdot}2 \times 10^4$ based on the width of the nozzle.

2. Apparatus, instrumentation and procedures

A blow-down-type air supply system was used to provide the airflow to a cylindrical settling chamber which was 1·75 m in length and 0·6 m in diameter. The facility was originally designed to provide sonic conditions at the exit plane of a nozzle for other experiments. Before reaching the nozzle, the air is passed through an adapter which contains six screens set 5 cm apart to reduce disturbances at the inlet of the nozzle. The ratio of areas between the adapter and the nozzle is 90, which is exceptionally

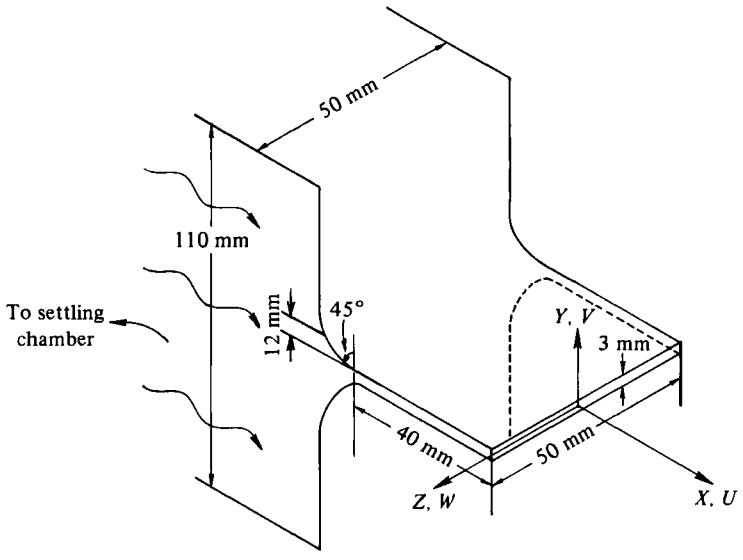

FIGURE 1. Schematic diagram of rectangular nozzle and entry region.

large when compared with the contraction ratio for conventional wind tunnels. The centre-line turbulence intensity at the exit of the nozzle was 0·3 per cent at a mean velocity of 60 m s^{-1}. In order to change the aspect ratio, the long (L) dimension of the rectangular nozzle was varied from 50 mm to 16·5 mm by introducing streamlined plugs into the nozzle. The short (D) dimension was fixed at 3 mm. The nozzle exit was preceded by a 40 mm long rectangular (50 × 3 mm) channel as shown in figure 1. The nozzle used is one of a multiple nozzle configuration which was designed to study the mixing of multiple rectangular jets.

Hot-wire measurements were made with DISA 55M01 constant-temperature anemometers in conjunction with DISA 55D10 linearizers. Most of the measurements were made using either an X-wire or a single wire. These wires were manufactured by DISA and constructed from 5 μm platinum-coated tungsten wire with an active length of 1·2 mm. Where X-probes were used, the attenuators on the linearizers were adjusted to give the same output for each wire when the probe was perfectly aligned with the stream. The yaw sensitivity of each wire was then checked by a calibration procedure. The simple cosine law was used to decompose the velocities. From the calibration data, it was evident that the use of the simple cosine law for an X-wire probe in turbulent flows has to be limited to situations where the angular rotation of the velocity vector does not exceed $\pm 25°$ (refer to Krothapalli 1979). In this angular range, the response of the hot wire was assumed known and no corrections resulting from higher-order terms were applied.

The two signals from the linearizers were sent through a sum and difference unit which was calibrated from d.c. to 100 kHz. The signals were then passed through a DISA type 55D31 digital voltmeter, a DISA type 55D35 r.m.s. unit, and a TSI model 1076 voltmeter to get the mean and r.m.s. values. The integration times on these instruments can be selected at discrete steps from 0·1 to 100 sec. Correlation measurements were made using an HP 3721A correlator. Measurements of the component spectra were obtained using an HP 8556A spectrum analyzer.

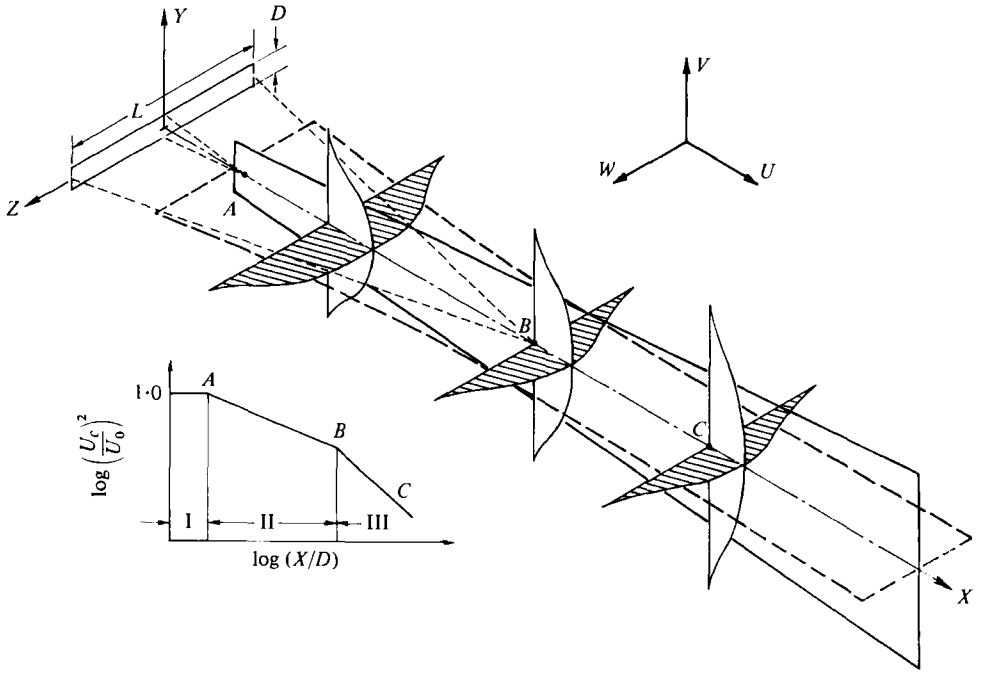

FIGURE 2. Schematic representation of the flow field of a rectangular jet.

A Cartesian co-ordinate system (X, Y, Z), as shown in figure 1, was chosen with its origin located at the centre of the nozzle and with X axis oriented along the centre-line of the jet. Hot-wire traverses were made in the two central X, Y and X, Z planes at various streamwise locations (X) covering up to $115D$. Unless otherwise stated, all the data presented here were taken with the X-wire probe. Mean velocity measurements were made across the entire jet in order to establish the symmetry of the flow about the central planes; however, only the data for each half-plane will be presented.

3. General features of the flow field

On the basis of the present investigation and the results reported by Sforza *et al.* (1966), Sforza & Stasi (1977), Sfeir (1976, 1978), and those summarized by Rajaratnam (1976), the flow field of a rectangular jet may be represented schematically as shown in figure 2. Also shown in the figure as an insert is the variation of $\ln (U_c/U_0)^2$ with $\ln X/D$, where U_c is the mean axial velocity along the centre-line of the jet and U_0 is the mean velocity at the centre of the nozzle exit. The three regions identified in the figure may be defined as follows: the first region is referred to as a potential core region in which the axial component of velocity is essentially a constant; the second region marked by AB, in which the velocity decays at a rate roughly the same as that of a planar jet, will be referred to as the two-dimensional region; and the third region, downstream of B, in which the velocity decays at nearly the same rate as that of an axisymmetric jet, will be referred to as an axisymmetric region. The two-dimensional-type region originates at about the location where the two shear layers in the X, Y plane (containing the short dimension of the nozzle) meet. Correspondingly,

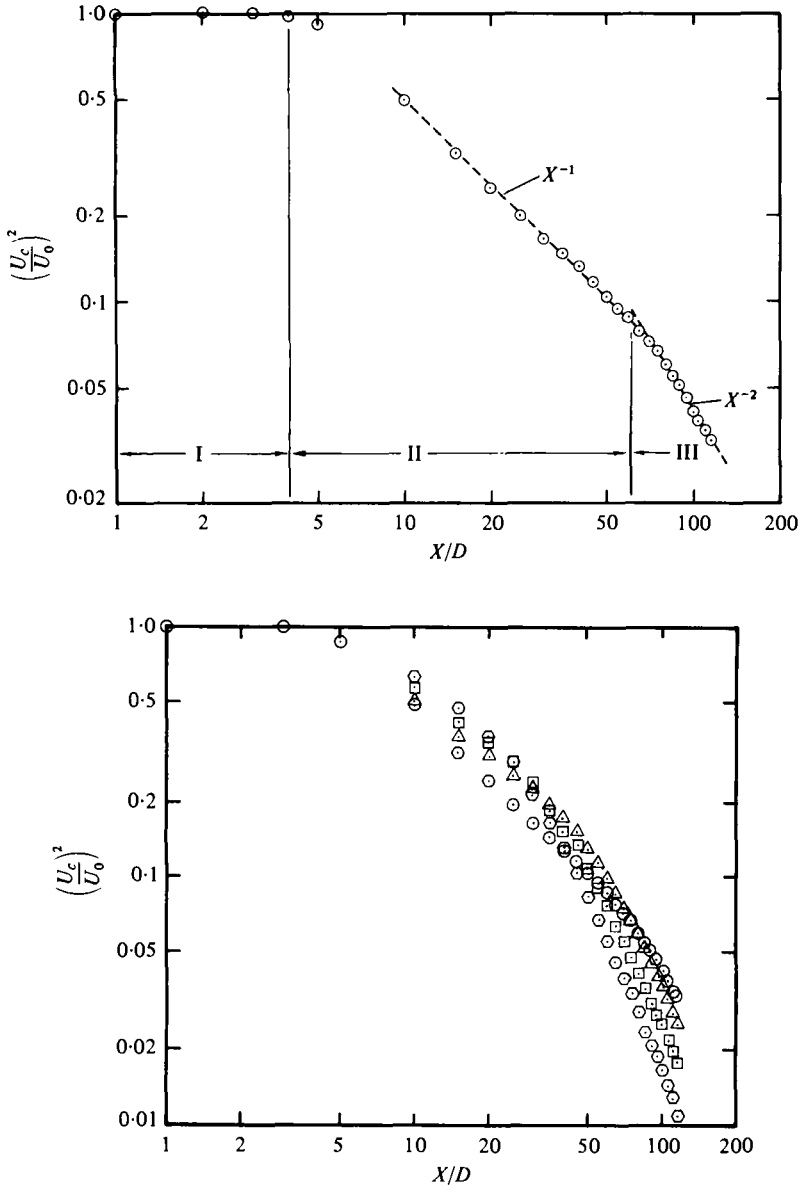

FIGURE 3. The decay of the axial mean velocity along the centre-line of the jet. (*a*) ○, $AR = 16{\cdot}7$, X-wire. (*b*) ○, $AR = 16{\cdot}7$; △, $AR = 12{\cdot}5$; □, $AR = 8{\cdot}3$; ⊙, $AR = 5{\cdot}5$.

one may expect the axisymmetric region to originate at the location where the two shear layers in the X, Z plane (containing the long dimension of the nozzle) would meet. This will be discussed later in the paper.

Profiles of the mean axial velocity in the X, Y and X, Z plane at three different locations are shown to scale in the schematic of the flow structure in figure 2. In regions I and II, the width of the jet in the X, Z plane is greater, as expected, than the width in the X, Y plane. At B, the widths in both planes are about the same. In region III, the width in the X, Y plane becomes larger than that in the X, Z plane.

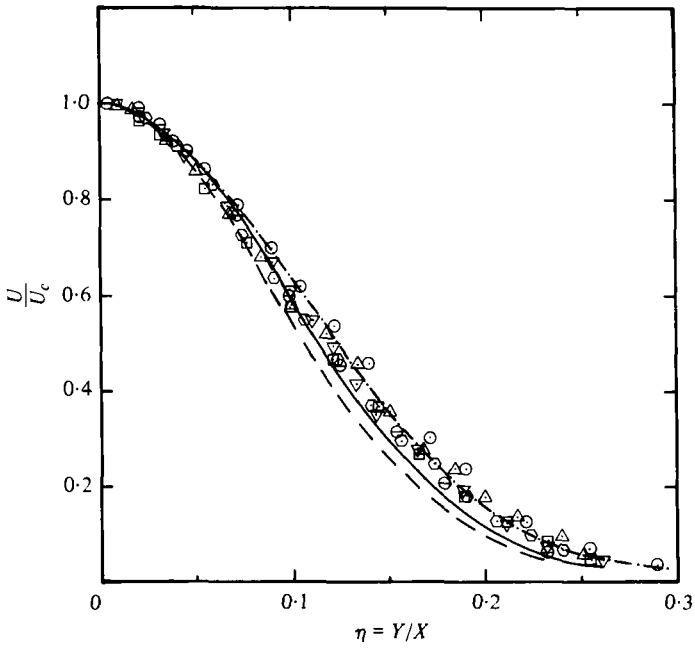

FIGURE 4. Axial mean velocity profiles in the X, Y plane, $Z = 0$. ⊙, $X/D = 20$; ▽, $X/D = 30$; △, $X/D = 40$; ⊡, $X/D = 60$; ⊙, $X/D = 80$; ⊖, $X/D = 100$; ——, $AR = 10$, Sfeir (1976); — —, $AR = 38$, Gutmark & Wygnanski (1976); — · —, $\exp[-0{\cdot}5(Y/Y_{\frac{1}{2}})^2]$.

The solid and dashed lines shown in the flow schematic depict the loci of maximum turbulent stresses in the two planes being considered. Further discussion of this will be given below.

4. Mean velocity field

Figure 3 (*a*) shows, for a nozzle of aspect ratio 16·7, the measured decay of the square of the axial mean velocity along the centre-line. The three regions introduced in figure 2 are noted as the potential core region which ends at approximately $4D$, the two-dimensional jet-type region extending up to about $60D$, and the axisymmetric jet-type region extending beyond $60D$. In the two regions II and III, U_c^2, indicated by the dashed lines, decays as X^{-1} and X^{-2}, respectively.

The extent of the regions (as shown in figures 2 and 3*a*) were shown by Trentacoste & Sforza (1967) and Sfeir (1976, 1978) to be functions of both the initial geometry and the aspect ratio of the nozzle. To identify the effects of aspect ratio on these regions, three additional nozzles of aspect ratio 5·5, 8·3, and 12·5 were tested. Results of the decay of the square of the mean axial velocity with downstream distance for these nozzles are shown in figure 3(*b*). As the aspect ratio decreases, the position of point B, that is, where the centre-line velocity first assumes an axisymmetric character, moves upstream toward the exit of the jet. From these measurements and the results of Sforza *et al.* (1966, 1977) and Sfeir (1976, 1978), one finds that, for nozzles of aspect ratio less than or equal to 10, U_c^2 in region II does not decay as X^{-1}. The exponent in this power law decay is dependent on orifice geometry, as shown by Sfeir (1978), and on the aspect ratio.

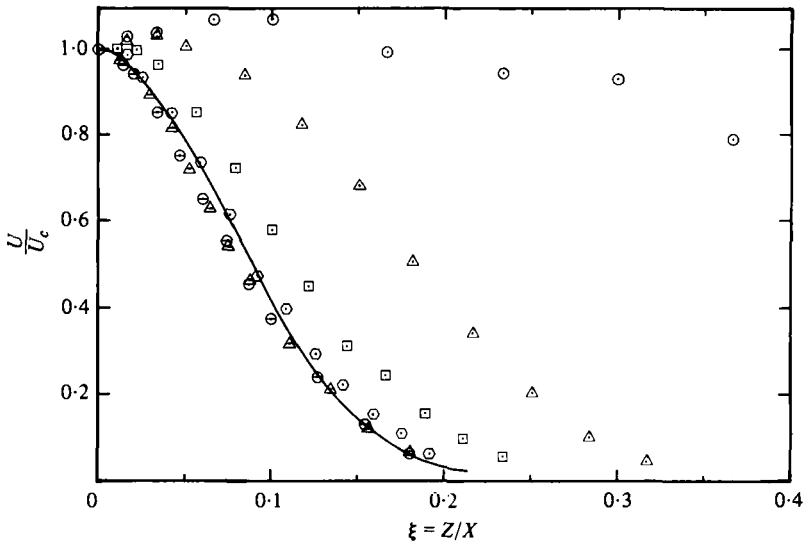

FIGURE 5. Axial mean velocity profiles in the X, Z plane. ○, $X/D = 20$; △, $X/D = 40$; ⊡, $X/D = 60$; ⊙, $X/D = 80$; ⊖, $X/D = 100$; ▲, $X/D = 115$; ——, axisymmetric jet, Wygnanski & Fiedler (1969).

Figure 4 shows the distribution of mean velocity U across the jet in the X, Y plane at different downstream stations, ranging from 20 to 100 widths. The velocity U is normalized with respect to U_c at each station, while the distance Y is normalized by the distance X to the station in question ($\eta = Y/X$). The profiles are geometrically similar, within the limits of error for the experiment, for X greater than or equal to $30D$. The results of Sfeir (1978) and Gutmark & Wygnanski (1976) for nozzle aspect ratios of 10 and 38, respectively, are plotted for comparison. The agreement between the three sets of data is good for η less than or equal to 0·1, but for η greater than 0·1 the profiles from the present investigation are somewhat wider than the rest. The shape of the profiles from these three sets of data seem to be similar. From these observations it appears that the aspect ratio does not play a critical role in determining the shape of the similarity profile in the X, Y plane, at least for aspect ratios greater than 10. However, Everett & Robins (1978) reported that the downstream distance where the profiles first assume self-similarity appears to be directly related to the nozzle aspect ratio. This similarity persists both in regions II and III as shown in the figure. Often one non-dimensionalizes the distance Y with respect to the local half-width of the jet $Y_{\frac{1}{2}}$ (the width corresponding to the point where the mean velocity is equal to one-half of its value on the axis). As discussed below, the half-width in the present investigation varies linearly with X. This being the case, the parameter η, but for a scale factor, represents equally the ratio $Y/Y_{\frac{1}{2}}$. For comparison purposes, the exponential function $\exp[-0{\cdot}5(Y/Y_{\frac{1}{2}})^2]$ of Reichardt's (1943) analysis for a two-dimensional jet is also shown in the figure and seems to agree satisfactorily with the present measurements.

Normalized axial mean velocity profiles in the X, Z plane for different downstream locations are shown in figure 5. The distance Z is again normalized with respect to the local longitudinal distance, $\xi = Z/X$. For locations X less than or equal to $60D$,

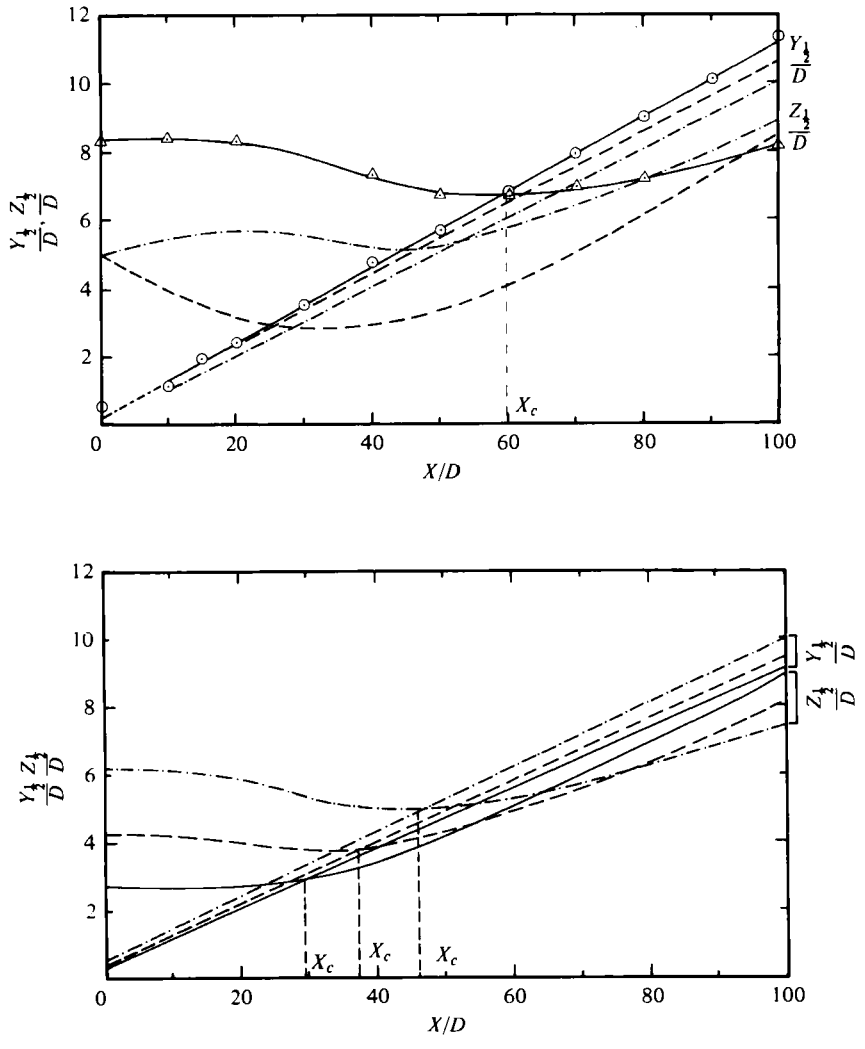

FIGURE 6. (*a*) Growth of a rectangular jet with downstream distance. ○, △, AR = 16·7, present measurements; — —, AR = 10, orifice-type nozzle, Sfeir (1976); — · —, AR = 10, channel-type nozzle, Sfeir (1976). (*b*) Effect of aspect ratio on growth of a rectangular jet. ——, AR = 5·5; — —, AR = 8·3; — · —, AR = 12·5.

profiles have a saddle shape with the maximum velocity occurring near the centre-line of the jet. The magnitude of the overshoot seems to be dependent on the type of initial geometry of the jet (Marsters 1979, private communication). This has also been noted by others (Sforza *et al.* 1966; Sforza & Stasi 1977; Sfeir 1976, 1978; Bradbury 1965; van Der Hegge Zigen 1958). As suggested by van Der Hegge Zigen (1958), such a profile may be explained as resulting from the superposition of a uniform stream with the flow due to a system of vortex rings representing the jet. However, more detailed study of the flow field is needed to understand clearly the origin of such profiles. At large distances downstream, i.e. for X greater than $80D$, the profiles appear to have a shape similar to that of an axisymmetric jet. The similarity profile of an axisymmetric jet reported by Wygnanski & Fiedler (1969) is shown for compari-

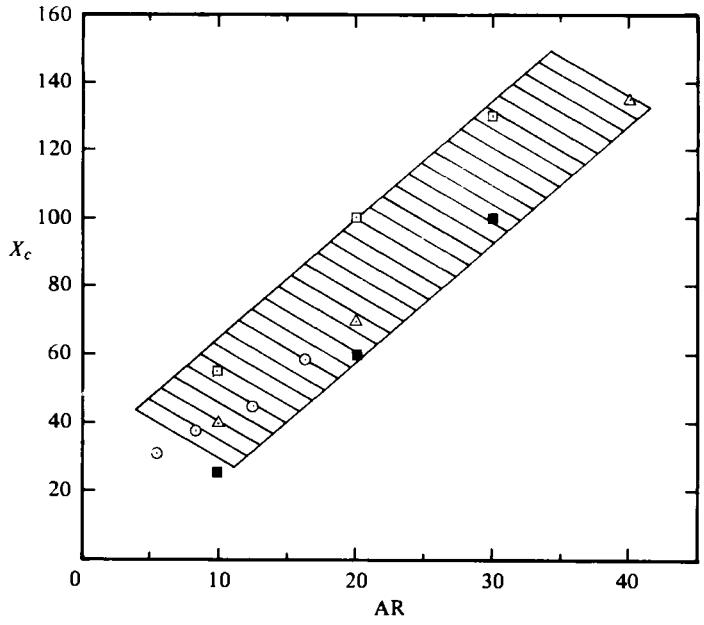

FIGURE 7. Variation of the cross-over point with aspect ratio. ⊙, present results; △, Sforza *et al.* (1966); ⊡, Sfeir (1976); ■, Sfeir (1976).

son. It is also observed from figures 4 and 5 that the velocity profiles at X equal to $60D$ in both planes are almost identical, and at this location the centre-line velocity first assumes the axisymmetric character. True axisymmetry (profiles are identical in both planes) of the mean velocity profiles was observed by Trentacoste & Sforza (1967) far downstream in the jet (i.e. for X greater than or equal to 150 for an aspect ratio of 10). In the present investigation, measurements are not made far enough downstream to confirm this.

The growth of the jet in X, Y and X, Z planes with downstream distance is shown in figure 6 (a). The ordinate $Y_{\frac{1}{2}}$ and $Z_{\frac{1}{2}}$ are the distances from the centre-line of the jet to the point where the axial mean velocity in each plane is equal to one-half of its centre-line values. The jet in the X, Y plane spreads linearly with X and the locus of the half-velocity points is given by

$$Y_{\frac{1}{2}} = k(X - X_0),$$

where $k = 0{\cdot}109$ and $X_0 = -2{\cdot}5D$. For planar jets, the value of k varies between 0·09 and 0·12, and a listing of these values for various experiments is given by Kotsovinos (1976). Similarly, the value of X_0 for the different experiments also varies. The variation of these constants can be attributed to different initial conditions and the free-stream turbulence level (Bradshaw 1966, 1977). As discussed later, these also depend upon the aspect ratio of the nozzle.

The variation of the half-width in the X, Z plane as shown in figure 6 (a) is neither linear nor does it increase monotonically. At some intermediate location ($X \simeq 60D$ for $AR = 16{\cdot}7$) the half-widths in the central planes cross over (this defines point B in figure 2). The distance from the nozzle exit to the cross-over point along the X axis is denoted by X_c. For comparison, the results of Sfeir (1978) for a nozzle aspect ratio

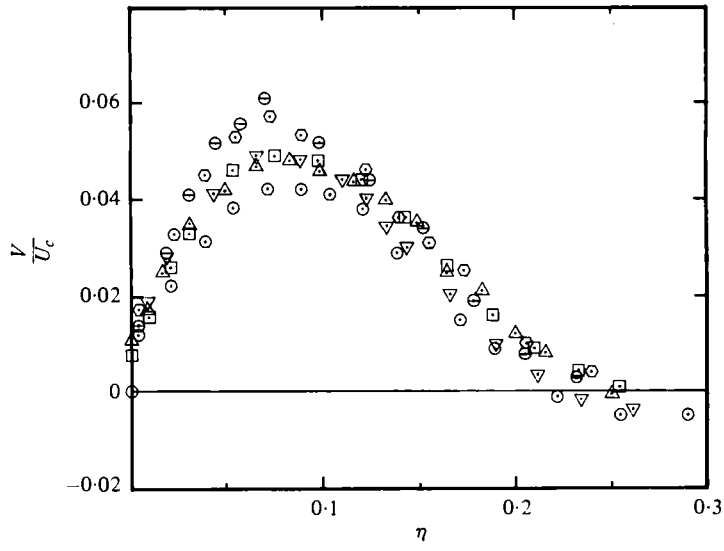

FIGURE 8. Lateral mean velocity profiles in the X, Y plane. Symbols as in figure 4.

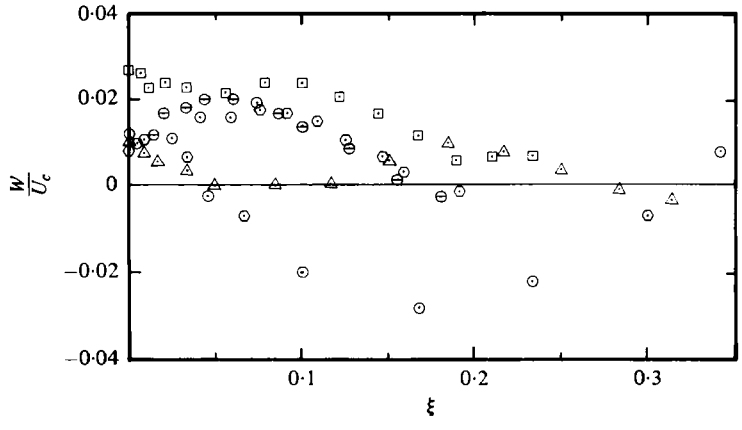

FIGURE 9. Transverse mean velocity profiles in the X, Z plane. Symbols as in figure 4.

of 10 and for different inlet geometries are shown in the figure. It is noted that $Y_{\frac{1}{2}}$ exhibits linear variation for different aspect ratios, although the slopes of the lines are different for different inlet geometries. Although the variation of $Z_{\frac{1}{2}}$ exhibits similar characteristics in the two studies, significant differences are found owing to different inlet geometries. It appears that the inlet geometry plays an important role in the development of the jet in the X, Z plane.

To observe the effect of aspect ratio on the growth of a jet, three additional aspect ratio nozzles were tested and the results are presented in figure 6 (*b*). It is observed that $Y_{\frac{1}{2}}$ exhibits linear variation for different aspect ratios, although the slopes of the lines are different for different aspect ratios. The variation of $Z_{\frac{1}{2}}$ exhibits similar characteristics for all four aspect ratios studied. As shown in the figure, the distance X_c (downstream location of the cross-over point) increases with aspect ratio.

The variation of X_c with aspect ratio is plotted in figure 7. The results of Sforza *et al.*

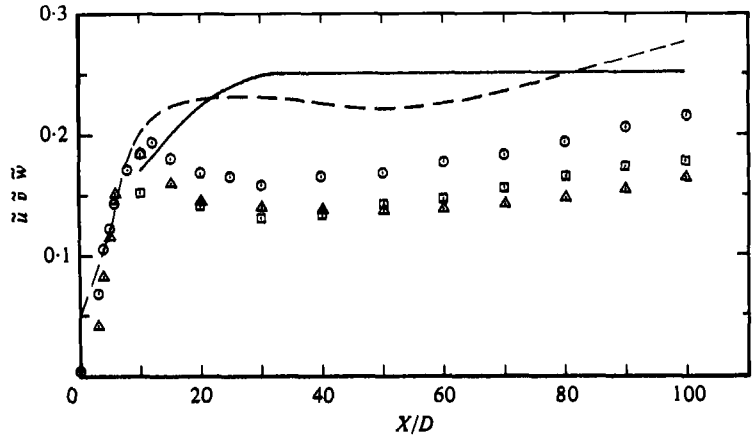

FIGURE 10. Variation of turbulent intensities along the centre-line of the jet. ⊙, $\tilde{u} = (\overline{u^2})^{\frac{1}{2}}/U_c$; △, $\tilde{v} = (\overline{v^2})^{\frac{1}{2}}/U_c$; ⊡, $\tilde{w} = (\overline{w^2})^{\frac{1}{2}}/U_c$; — —, $\tilde{u}$, $AR = 10$, Sfeir (1976); ——, $AR = 38$, Gutmark & Wygnanski (1976).

(1966) and Sfeir (1976) are also included in the figure. From the data of Sfeir it appears that, for a given aspect ratio, X_c appears further downstream for a jet exiting from a long channel than for a jet exiting from an orifice. This indicates that X_c depends strongly on the character of the initial flow. For aspect ratios greater than 10, it appears that X_c varied linearly with X as shown by the shaded region.

The mean lateral velocities in the two central planes were measured and the results are shown in figures 8 and 9. These velocities are a small fraction (5–6 %) of the mean axial velocity; thus an experimental accuracy of about 20 per cent was the best attained. Furthermore, large errors are inherent in using hot-wire anemometry in the outer regions of the jet. Profiles of the mean velocity V in the central X, Y plane for different downstream locations are shown in figure 8. They are geometrically similar for $30D \leqslant X \leqslant 60D$ and have the expected distribution. Very little mean entrained flow (indicated by the negative V component of velocity) is found in the outer region of the jet for X greater than $20D$.

The mean W component of velocity in the central X, Z plane for different downstream locations is plotted in figure 9. For much of the profile at X equal to $20D$, the W component of velocity points toward the axis of the jet (indicated by the negative values). More detailed measurements in the entire cross-sectional plane and at the exit plane of the jet are required to interpret these results properly. Owing to the limitation on the dimensions of the probe, with respect to the nozzle, measurements were made for X greater than $10D$.

5. R.m.s. intensities and shear stresses

The r.m.s. values of the three components of velocity on the centre-line of the jet are shown in figure 10. These values are normalized with respect to the local mean axial velocity on the centre-line. The magnitude of $\tilde{u}$ ($\tilde{u} = \overline{u^2}^{\frac{1}{2}}/U_c$) increases sharply close to the jet exit and reaches a maximum value of about 0·195 at X equal to $10D$. It then decreases and increases again gradually. Such a behaviour, for X less than $30D$, is typical of a jet with laminar top-hat profile (starting boundary layers are

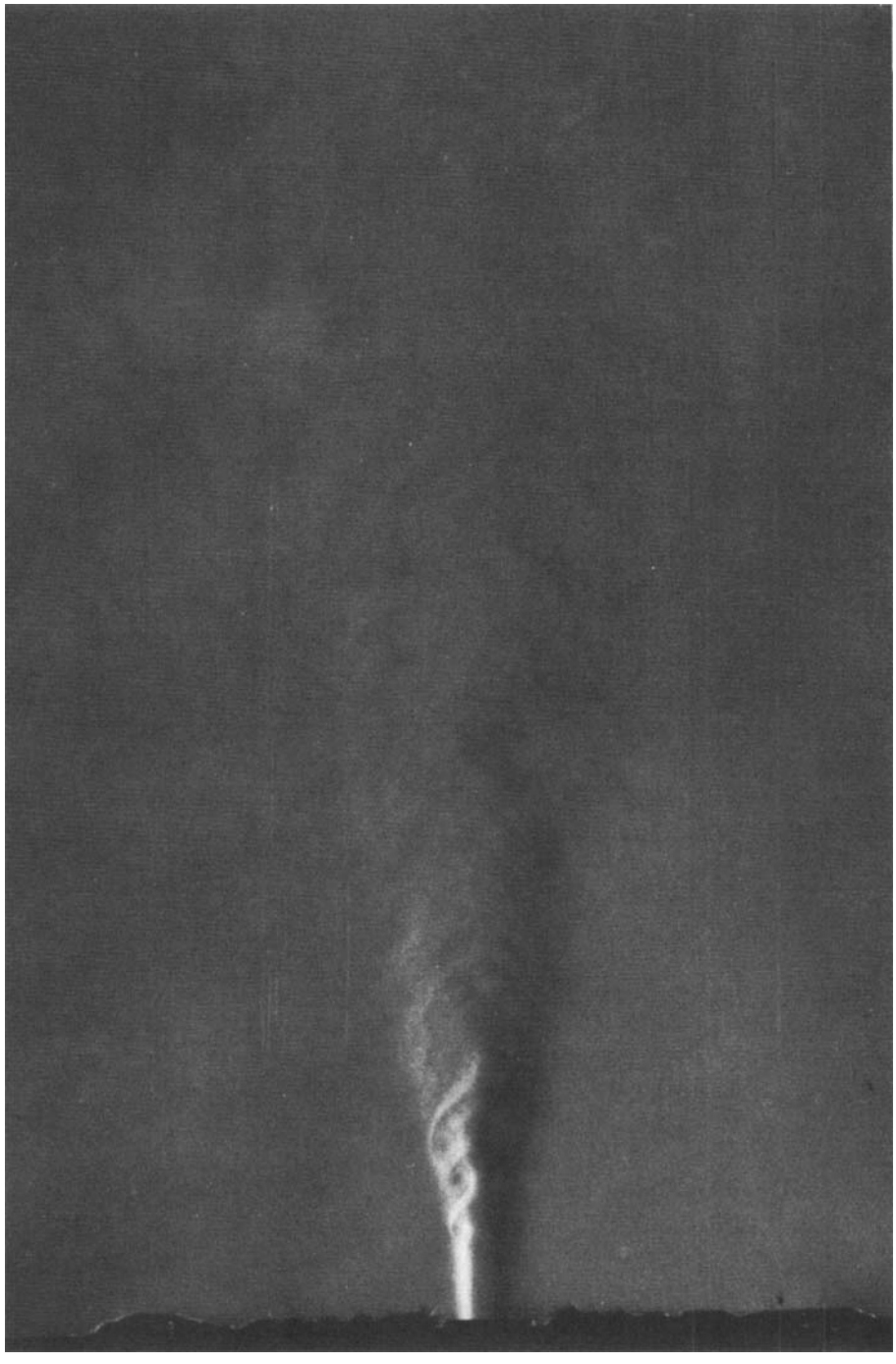

FIGURE 11. Schlieren picture of the jet in the X, Y plane.

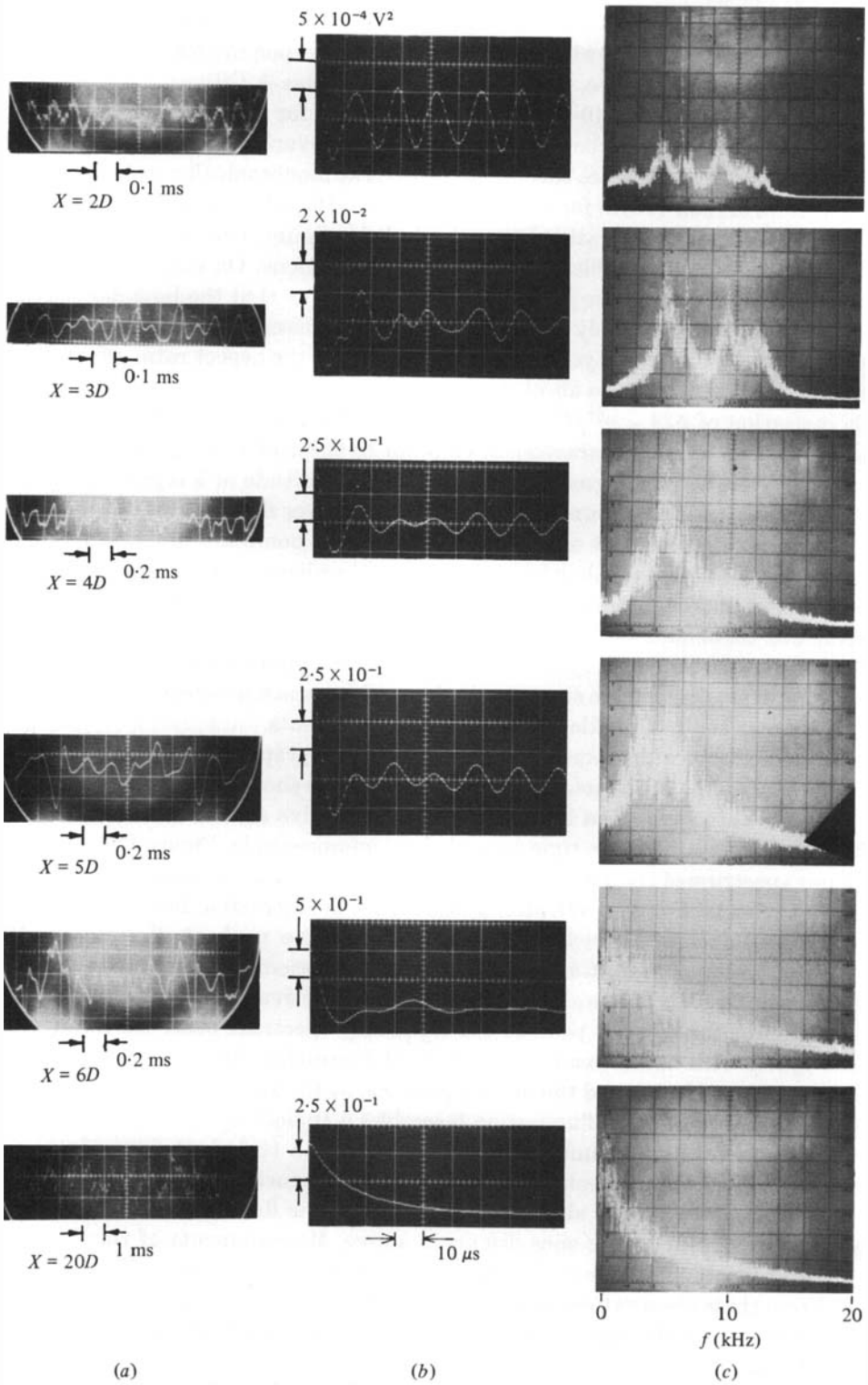

FIGURE 12. (*a*) Signal, (*b*) autocorrelation, (*c*) spectrum, of u fluctuations along the centre-line of the jet.

laminar) at the exit plane and which goes through a transition region before it becomes a turbulent jet. This has been observed by Sato (1960) for a two-dimensional jet. The variation of $\tilde{u}$ with X has been observed to depend upon the state of the boundary layers at the nozzle exit. See, for instance, Hill, Jenkins & Gilbert (1976) for a rectangular jet of aspect ratio 10·5 and Bradshaw (1966) for an axisymmetric jet. They found that, when the boundary layers are laminar, $\tilde{u}$ varies as discussed above while when the boundary layers are turbulent, $\tilde{u}$ varies as monotonically with X.

The results of Sfeir (1978) for a jet of aspect ratio 10 and those of Gutmark & Wygnanski (1976) for an aspect ratio of 38 are included in figure 10 for comparison. In both cases, the exit velocity profiles were top-hat distributions. On examining the variations of $\tilde{u}$ with X close to the jet exit, one may conclude that the boundary layers in these two cases were probably turbulent. From these observations, we note that both the state of the boundary layer at the nozzle exit and the aspect ratio affect the way $\tilde{u}$ varies with X as well as its absolute magnitude.

The variation of $\tilde{v}$ ($\tilde{v} = \overline{v^2}^{\frac{1}{2}}/U_c$) and $\tilde{w}$ ($\tilde{w} = \overline{w^2}^{\frac{1}{2}}/U_c$) along the centre-line, as shown in figure 10, also exhibit characteristics similar to those of $\tilde{u}$. In the fully developed region of the jet, i.e. for X greater than $30D$, the magnitude of $\tilde{u}$ is greater than that of either $\tilde{v}$ or $\tilde{w}$, as is also found in other free shear layer flows.

In investigating the effect of the state of the initial boundary layer on jet mixing, Hill *et al.* (1976) studied the flow by means of spark schlieren photographs. They found coherent large-scale structures in the jet shear layer when the initial layer was laminar. When it was turbulent, such structure was not observed. A typical schlieren picture (with an exposure time of 1·5 μs) of the jet flow in the present investigation is shown in figure 11. Here, large-scale structure is observable, as in the case of Hill *et al.* (1976), for the laminar top-hat profile present in the experiments.

To examine further the large-scale structure, oscillograph records of $\tilde{u}$ fluctuations along the centre-line of the jet, for $2D \leqslant X \leqslant 20D$, are shown in figure 12 (*a*). Oscillograms of the autocorrelation function for the respective signals are shown in figure 12 (*b*), where the scale for the time variable is in microseconds. Figure 12 (*c*) shows the frequency spectrum of the u fluctuations along the centre-line of the jet. The horizontal scale is in kilohertz. For $X < 4D$, strong periodicity is observed in both the time signal and the autocorrelation function. A strong distinctive peak at X equal to $4D$ is observed in the spectrum at about 5800 Hz. Some periodicity remains in the signal for stations up to $10D$. This is also shown by their respective autocorrelation functions. The position of the distinct peak in the frequency spectrum observed for $X < 10D$ moves slightly with downstream distance. With increasing distance downstream, the spectral energy shifts toward the low frequencies, as shown in the figure. At $20D$, the oscillograph record of the u fluctuation resembles a typical signal in a turbulent flow field. The autocorrelation function is also typical of a turbulent flow. Most of the energy in the frequency spectrum is in the low frequencies (i.e. less than 10 kHz). Similar measurements were also made for the v and w fluctuations and the results show features similar to the ones discussed above. Measurements of this kind were also made at locations off the centre-line of the jet, and no significant differences were found. From these observations along with the schlieren pictures, one may conclude that discrete frequencies appear only in the initial stages of transition from laminar to turbulent flow.

Profiles in the X, Y plane of $\tilde{u}$, $\tilde{v}$, and $\tilde{w}$ at different downstream locations X are

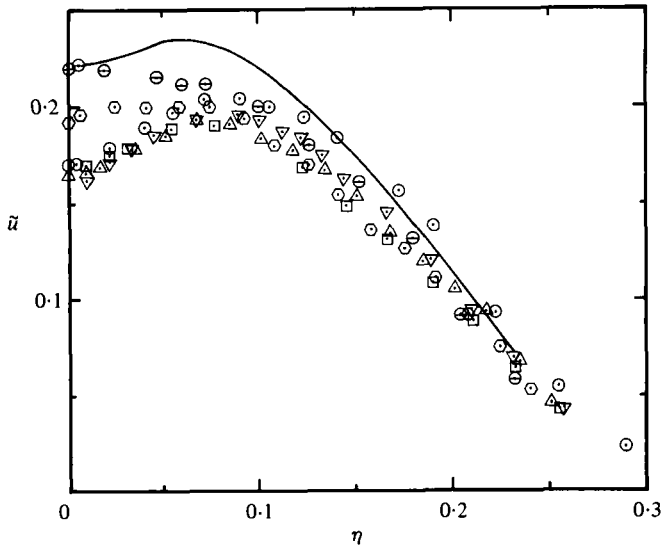

FIGURE 13. Distribution of the axial velocity fluctuations in the X, Y plane, symbols as in figure 4; ——, Everett & Robins (1978).

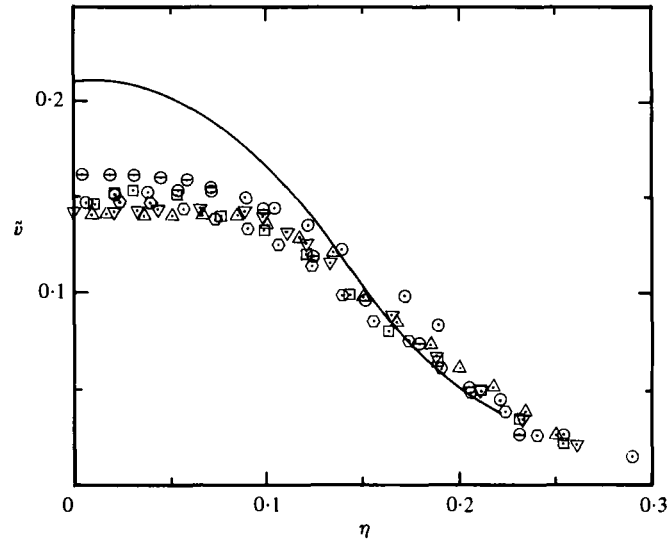

FIGURE 14. Distribution of the lateral velocity fluctuations in the X, Y plane, symbols as in figure 4; ——, Everett & Robins (1978).

shown in figures 13–15. The $\tilde{u}$ profiles indicate geometrical similarity for $30D \leqslant X \leqslant 60D$ and show a distinct saddle shape. Similar measurements have been made by Sfeir (1978). After careful examination of his data and in light of the present measurements, it is noted that both sets of data (see Sfeir 1978, and the present investigation) are similar only in the so-called two-dimensional region of the jet (see region II of figure 2). The maximum value of $\tilde{u}$ occurs at $\eta \simeq 0{\cdot}075$. The $\tilde{u}$ profiles for two-dimensional jets show fairly large variations from one investigation to another (see figure 5 of Everett & Robins 1978). A typical profile of Everett & Robins (1978) is plotted for comparison.

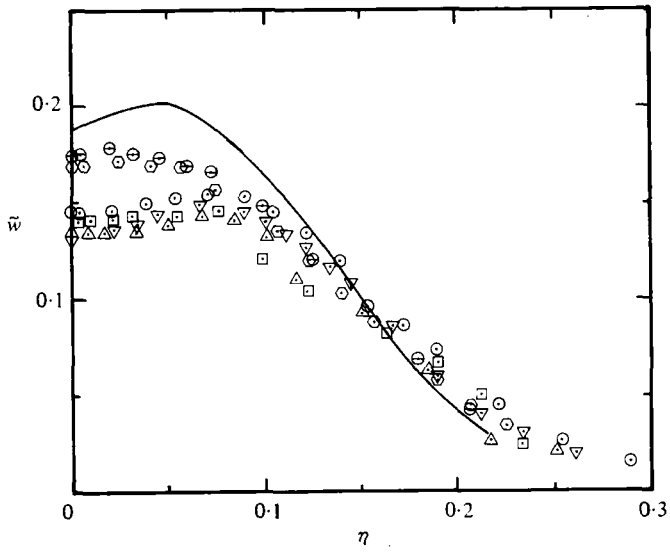

FIGURE 15. Distribution of the transverse velocity fluctuations in the X, Y plane, symbols as in figure 4; ——, Everett & Robins (1978).

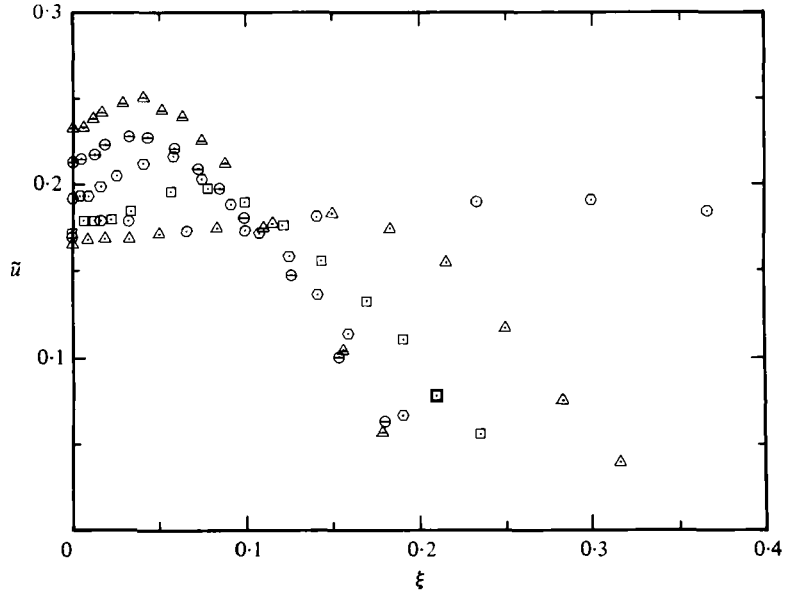

FIGURE 16. Distribution of the axial velocity fluctuations in the X, Z plane, symbols as in figure 5.

In general, the shape of the profile agrees with present measurements. For locations of X greater than $60D$ (i.e. in the so-called axisymmetric region) the profiles assume an axisymmetric character (see figure 4 of Wygnanski & Fiedler 1969).

The profiles of $\tilde{v}$ and $\tilde{w}$ are shown in figures 14 and 15, respectively. In the two-dimensional region, each of these profiles shows behaviour similar to that of a two-dimensional jet.

Profiles of $\tilde{u}$, $\tilde{v}$ and $\tilde{w}$ in the X, Z plane are shown in figures 16–18. It appears when

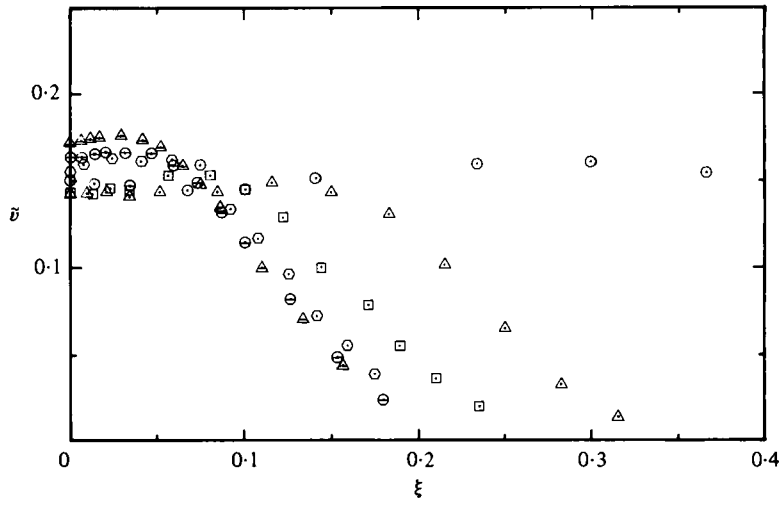

FIGURE 17. Distribution of the lateral velocity fluctuations in the X, Z plane, symbols as in figure 5.

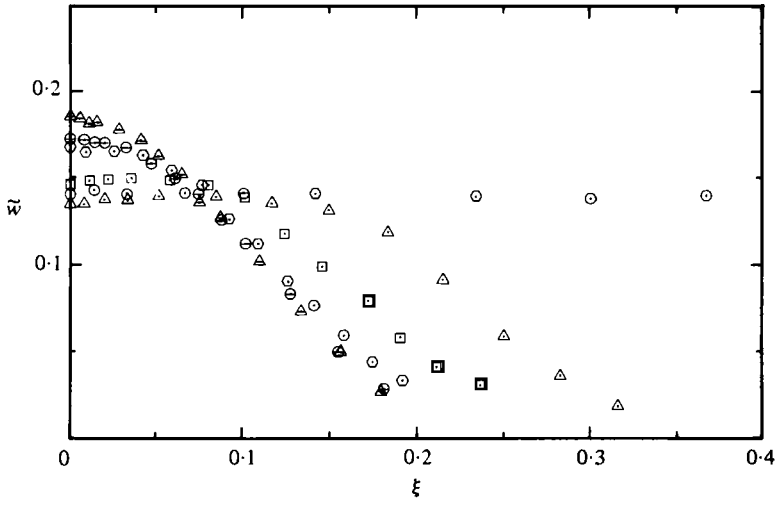

FIGURE 18. Distribution of the transverse velocity fluctuations in the X, Z plane, symbols as in figure 5.

comparing the $\tilde{u}$ profiles in figure 16 with the corresponding mean-velocity profiles in figure 5 that the point of maximum turbulence intensity coincides with the point where the velocity gradient $(\partial U/\partial z)$ is maximum. The $\tilde{u}$ profile in the X, Z plane develops a strong saddle shape for X greater than $60D$ as shown in the figure. The appearance of a saddle-shape profile in a jet usually indicates the end of the so-called potential core, which marks the merging of the two shear layers of the jet. With this in mind, it may be argued that the two shear layers separated by the long dimension of the nozzle, in the present investigation, meet at $X \simeq 60D$.

The profiles of $\tilde{v}$ and $\tilde{w}$ in the X, Z plane are shown in figures 17 and 18, respectively. At each downstream location, the magnitudes of $\tilde{v}$ and $\tilde{w}$ are about the same at their corresponding positions in the lateral direction (i.e. along the Z axis).

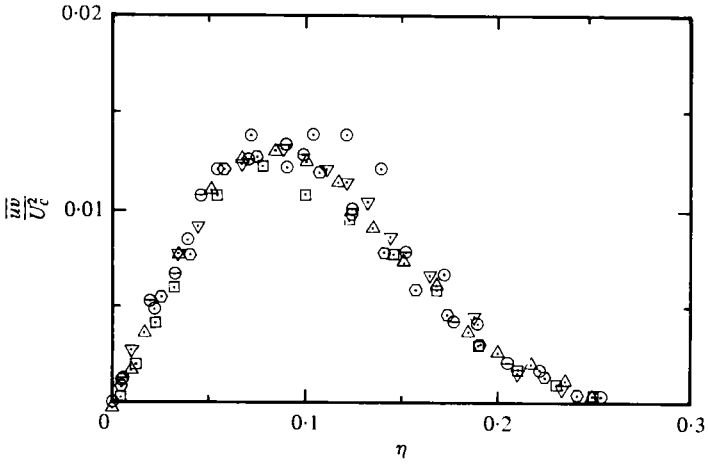

FIGURE 19. Distribution of the turbulent shear stress in the X, Y plane, symbols as in figure 4.

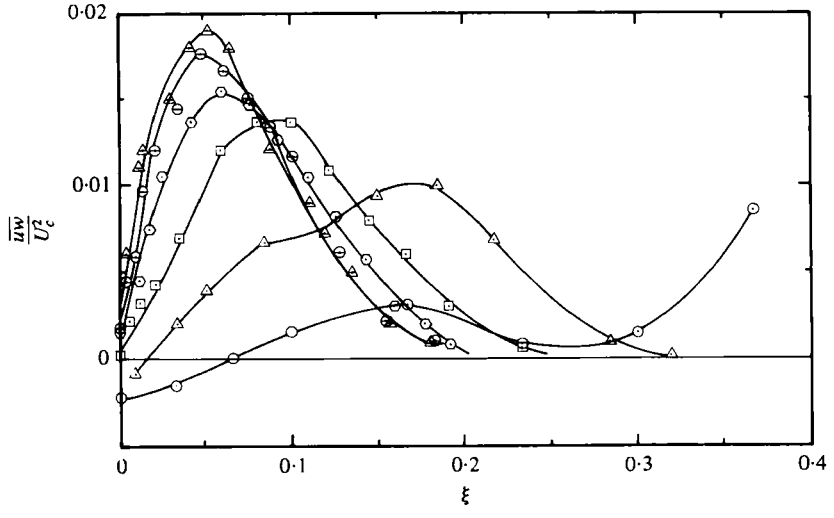

FIGURE 20. Distribution of the turbulent shear stress in the X, Z plane, symbols as in figure 5.

The normalized turbulent shear stress $\widetilde{uv}$ ($\overline{uv}/U_c^2$) in the X, Y plane for different downstream locations is shown in figure 19. The stress is normalized with respect to the square of the local centre-line velocity. The profiles are geometrically similar for X greater than or equal to $30D$. The maximum value is observed at $\eta \simeq 0{\cdot}075$, and this is also where the gradient $(\partial U/\partial y)$ and the turbulent energy in region II were found to be maximum. The magnitude of the normalized turbulent shear stress $\widetilde{uw}$ ($\overline{uw}/U_c^2$) was found to be much less than that of $\widetilde{uv}$ at corresponding locations in the X, Y plane and is not presented here.

Figure 20 shows the normalized shear stress $\widetilde{uw}$ profiles in the X, Z plane. At each location X, the point of maximum shear stress corresponds to the point of maximum velocity gradient $(\partial U/\partial z)$ and the point of maximum turbulent energy. In region III,

at any given X, the magnitude of the maximum $\widetilde{uw}$ in the X, Z plane is found to be greater than the maximum $\widetilde{uv}$ in the X, Y plane (see figures 19 and 20). At each location X, for both the X, Y and X, Z planes, the point of maximum shear stress corresponds to the point of maximum $\tilde{u}$, $\tilde{v}$ and $\tilde{w}$. The loci of these points are shown in the flow diagram of figure 2.

6. Concluding remarks

In the case of a single rectangular jet, the flow is characterized by the presence of three distinct regions when the decay of the square of the axial mean velocity along the centre-line of the jet is used to describe the flow field. These regions are: the potential core region, a two-dimensional-type region, and an axisymmetric-type region. The onset of the second region appears to be at a location where the shear layers separated by the short dimension of the nozzle meet. Correspondingly, the centre-line velocity decay first assumes the axisymmetric character at a location where the two shear layers separated by the long dimension of the nozzle meet.

The following conclusions can be drawn from the measurements in the central X, Y plane of the jet. The mean velocity and the shear stress ($\widetilde{uv}$) profiles show similarity about 30 widths downstream from the nozzle exit. There is some evidence that the shape of the profile may not depend upon the aspect ratio of the nozzle. However, the downstream distance where the profile first assumes similarity appears to be related to the nozzle aspect ratio. The half-width of the jet varies linearly with downstream distance, with different slopes for different aspect ratios, and initial geometries. The r.m.s. velocity profiles show similarity in the second region (i.e. two-dimensional region) but not in the third region (i.e. the axisymmetric-type region).

From the measurements in the central X, Z plane, the following conclusions are drawn. For X less than $60D$, the profiles of axial mean velocity exhibit a saddle shape, while the profiles in region III approach the similarity profile of an axisymmetric jet. For X less than $40D$, the profiles of transverse mean velocity (W) exhibit strong negative values along the Z axis. To interpret these results properly, a detailed map of the entire flow field is necessary. The r.m.s. velocity, and the shear stress ($\widetilde{uw}$) profiles do not exhibit similarity for downstream stations measured.

The present investigations, as described, furnish detailed experimental data which, on one hand, support some of the previous observations such as those of Sforza and coworkers and Sfeir while, on the other hand, are more extensive than those. Sforza and his coworkers' studies were concerned mainly with Pitot tube measurements and thus with mean profiles. Sfeir made hot-wire measurements of U, $\tilde{u}$, $\tilde{v}$, $\tilde{w}$ and $\widetilde{uv}$ in the X, Y plane and of $\tilde{u}$ only in the X, Z plane. No measurements of either V or W, or of the detailed turbulent structure in the Y, Z plane have been reported previously, but are now given. Furthermore, except for the geometrical description of the nozzle configurations used, adequate knowledge of the flow conditions at the nozzle exit such as the velocity profile, nature of the boundary layer and the initial turbulence intensities was not previously available. The importance of the nozzle exit flow condition is brought out in the present studies.

The present studies are still not complete enough to enable a detailed understanding of the complex flow development of the jet issuing from a rectangular nozzle of moderate aspect ratio. All the implications of the results obtained are not yet fully

understood. Further detailed investigations are clearly needed to clarify the importance of the flow details at the nozzle exit and the flow structure close to it. In the present investigations, the boundary layer is laminar at the nozzle exit. With a turbulent boundary layer, the flow structure close to the exit would certainly be different from that with the laminar layer and is likely to significantly affect the later development of the jet. Studies in this direction are needed. Finally, measurements in planes other than the X, Y and X, Z planes are required to properly characterize and elucidate the flow structure.

This work was supported by NASA Ames Research Centre. It is a pleasure to thank Mr David Hickey for his helpful suggestions and encouragement throughout this work.

REFERENCES

BOBBA, R. C. & GHIA, N. 1979 A study of three dimensional compressible turbulent jets. *2nd Symp. on Turbulent Shear Flows, Imperial College, London.*

BRADBURY, L. J. S. 1965 The structure of a self-preserving turbulent plane jet. *J. Fluid Mech.* **23**, 31–64.

BRADSHAW, P. 1966 The effect of initial conditions on the development of a free shear layer. *J. Fluid Mech.* **26**, 225–336.

BRADSHAW, P. 1977 Effects of external disturbances on the spreading rate of a plane turbulent jet. *J. Fluid Mech.* **80**, 795–797.

EVERETT, W. K. & ROBINS, G. A. 1978 The development and structure of plane jets. *J. Fluid Mech.* **88**, 563–584.

GUTMARK, E. & WYGNANSKI, I. 1976 The planar turbulent jet. *J. Fluid Mech.* **73**, 465–495.

HILL, G. W., JENKINS, C. J. & GILBERT, B. L. 1976 Effects of initial boundary layer state on turbulent mixing. *A.I.A.A. J.* **14**, 1513–1514.

HINZE, J. O. 1976 *Turbulence*, 2nd edn. McGraw-Hill.

KOTSOVINOS, E. N. 1976 A note on the spreading rate and virtual origin of a plane turbulent jet. *J. Fluid Mech.* **77**, 305–311.

KROTHAPALLI, A. 1979 An experimental study of multiple jet mixing. Ph.D. dissertation, Stanford University.

MCGUIRK, J. J. & RODI, W. 1977 The calculation of three-dimensional turbulent shear flows. *1st Symp. on Turbulent Shear Flows, Pennsylvania State University.*

RAJARATNAM, N. 1976 *Turbulent Jets.* Elsevier.

REICHARDT, H. 1943 On a new theory of turbulence. *J. Roy. Aero. Soc.* **47**.

SATO, H. 1960 The stability and transition of a two-dimensional jet. *J. Fluid Mech.* **7**, 53–55.

SCHLICHTING, H. 1968 *Boundary Layer Theory*, 6th edn. McGraw-Hill.

SFEIR, A. A. 1976 The velocity and temperature fields of rectangular jets. *Int. J. Heat Mass Transfer* **19**, 1289–1297.

SFEIR, A. A. 1978 Investigation of three-dimensional turbulent rectangular jets. *AIAA Paper* no. 78–1185.

SFORZA, M. P., STEIGER, H. M. & TRENTACOSTE, N. 1966 Studies on three-dimensional viscous jets. *A.I.A.A. J.* **4**, 800–806.

SFORZA, M. P. & STASI, W. 1977 Heated three-dimensional turbulent jets. *A.S.M.E. Publication* 77-WA/HT27.

TOWNSEND, A. A. 1976 *The Structure of Turbulent Shear Flow.* Cambridge University Press.

TRENTACOSTE, N. & SFORZA, M. P. 1967 Further experimental results for three-dimensional free jets. *A.I.A.A. J.* **5**.

VAN DER HEGGE ZIJEN, G. B. 1958 Measurements of the velocity distribution in a plane turbulent jet of air. *Applied Scientific Research* A **7**, 256–292.

WYGNANSKI, I. & FIEDLER, H. 1969 Some measurements in the self-preserving jet. *J. Fluid Mech.* **38**, 517–612.